Structural stability test of hexagonal $CePO_4$ nanowires synthesized at ambient temperature

P. Pusztai[1], T. Simon[1], Á. Kukovecz[1,2], Z. Kónya[1,3]

[1]Department of Applied and Environmental Chemistry, University of Szeged, H-6720 Szeged, Rerrich Béla tér 1., Hungary

[2]MTA-SZTE "Lendület" Porous Nanocomposites Research Group, H-6720 Szeged, Rerrich Béla tér 1., Hungary

[3]MTA-SZTE Reaction Kinetics and Surface Chemistry Research Group, H-6720 Szeged, Rerrich Béla tér 1., Hungary

Abstract

Until now one-dimensional $CePO_4$ nanostructures were investigated mainly from the characterization and photoluminescent property improvement point of view. In this study we present a structural stability test of $CePO_4$ nanowires prepared at ambient temperature. The calcination of the nanowires was carried out at 400 °C, 600 °C, 800 °C and 1000 °C for one hour in air atmosphere, the morphological and surface changes were monitored by transmission electron microscopy (TEM) and nitrogen adsorption technique. An increasing tendency in average diameter and a decreasing tendency in specific surface area were identified indicating a sintering process above 600 °C. The phase transition of the nanowires was investigated by X-ray diffraction (XRD), Raman and infrared spectroscopy. The XRD study showed the recrystallization of the nanowires from hexagonal to monoclinic phase at 600 °C which was further confirmed by Raman and IR spectroscopy.

Introduction

In recent years one-dimensional nanomaterials became one of the most investigated area in materials science as their novel properties associated with their reduced dimensionality opened new frontiers for their application in advanced electronic, optoelectronic, electrochemical and electromechanical devices [1, 2]. Since the discovery of nanowires, nanotubes, nanobelts etc. considerable efforts have been made for the development of simple and reproducible synthetic routes for the controlled preparation of inorganic one-dimensional nanomaterials. Polyol, sonochemical, microemulsion, chemical vapor deposition and hydrothermal methods are the most frequently applied techniques for the morphological manipulation of materials in nanoscale.

Beyond various inorganic nanomaterials the fabrication of rare-earth compounds has received much attention due to their potential applications in magnets, catalysts, various displays, biochemical labeling of cells etc [3,4,5,6,7]. In particular, cerium-phosphate is a rare-earth compound which can be easily utilized for the development of highly efficient photoluminescent devices using various cations as dopants [8]. These can be applied in luminescent biological labeling [9], as catalyst [10,11], or as a container material of nuclear waste [12,13]. Their cation exchange properties can be utilized for the removal of toxic cations from wastewater [14,15] or they can be used as a proton conduction electrolyte in solid oxide fuel cells [16].

For the preparation of pure cerium-phosphate nanowires several synthetic procedures can be found in the literature, for instance sonochemical [17], microemulsion [18] and hydrothermal methods [19]. These methods can be also applied for the fabrication of various rare-earth cation doped or core/shell cerium-phosphate nanowires with enhanced photoluminescent properties [20,21]. The readiness of cerium-phosphate to grow into one dimensional nanostructures is due to the anisotropic growth nature of seed hexagonal crystal structure [9].

The available open literature focuses mostly on the synthesis, characterization and improvement of the optical properties of cerium-phosphate nanowires. It is well known that cerium-phosphate nanowires possess improved photoluminescent properties (especially when doped with Tb^{3+}cations [22]) which can be utilized for the development of advanced photoluminescent devices and displays. Considering their low toxicity and high stability, they can be used as a bioimaging material as well [9]. Microstructure studies have already been published on $CePO_4$ [23,24] however, only a few reports are available on the structural stability of the nanowire form of this material [25].

In this paper we report on the structural stability test of $CePO_4$ nanowires applying elevated temperatures. The structural changes and phase transitions were followed by high resolution transmission electron microscopy, X-ray diffractometry, Raman and Infrared spectroscopy.

1. Experimental

2.1. Materials

Analytical grade $Ce(NO_3)_3 \cdot 6H_2O$ (puriss $\geq$ 99.0%) was purchased from Sigma-Aldrich, H_3PO_4 (85%) and absolute ethanol were purchased from Molar Chemicals Ltd. All chemicals were used without further purification. The reactions were carried out in 120 ml Teflon-lined stainless steel autoclaves put into a digital-type temperature-controlled oven.

2.2. Synthesis of $CePO_4$ nanowires

For the preparation of $CePO_4$ nanowires we used a simple, easily scalable, room-temperature synthesis method which was recently developed in our laboratory (**Hiv: Pusztai et.al. in preparation)**. In a typical procedure 240 ml of $Ce(NO_3)_3 * 6H_2O$ and 80 ml of H_3PO_4 aqueous solutions were prepared with a concentration of 0.033 M and 0.2 M respectively. The H_3PO_4 solution was added dropwise to the $Ce(NO_3)_3 * 6H_2O$ solution under vigorous stirring. After an additional 20 minutes of stirring the white precipitate was collected by centrifugation and washed with distilled water and ethanol several times. Finally, the $CePO_4$ nanowires were obtained by drying the sample at 60°C overnight.

For the structural stability test 4 x 200 mg of the as prepared nanowires were subjected to a calcination process performed at the temperature range of 400 – 1000 °C for 1 hour.

2.3. Characterization

The crystal characteristics of the as-prepared and calcined nanowires were determined by X-ray diffraction, Raman and Infrared measurements. An XRD study was carried out on a Rigaku Miniflex II powder X-ray diffractometer equipped with a Cu Kα radiation source (λ = 0.15418 nm) by applying a scanning rate of 1°/min in the 2θ range of 10° - 70°. The ambient temperature Raman spectra were collected with a Thermo Scientific DXR Raman Microscope in the range of 200 – 1400 cm^{-1} with a resolution of 4 cm^{-1} using a 532 nm excitation laser. The infrared absorption spectra were recorded on a Bruker Vertex 70 FTIR instrument in the range of 400 – 1400 cm^{-1} with a spectral resolution of 4 cm^{-1}. For infrared measurements the KBr pellet technique was

applied. High resolution electron microscopy was carried out to monitor the structural changes of the calcined nanowires using a FEI TECNAI G^2 20 X-Twin HRTEM working at an accelerating voltage of 200 kV. The samples for TEM measurements were drop-casted onto carbon coated copper grids from ethanol suspension. The purity of the as-prepared samples was verified using energy dispersive X-ray spectroscopy (EDS) in a HITACHI S-4700 Type II cold field emission SEM instrument operated at 10 or 20 kV accelerating voltage with an integrated Röntec QX2 EDS detector. Samples were mounted on double-sided adhesive carbon tape. Nitrogen adsorption measurements were carried out on a Quantachrome NOVA 3000e surface area and pore size analyzer instrument. The samples were degassed at 200 °C for 2 hours.

3. Results and discussion

TEM, XRD, electron diffraction (ED) and EDS were utilized to assess the morphology, crystallinity and purity of the nanowires..The TEM image depicted in Fig. 1. indicates that the sample consists of several hundred nanometer long nanowires. The sharp circles in the corresponding ED pattern prove the crystalline nature of the nanowires. The XRD pattern of the sample showed all the characteristic peaks of the hexagonal $CePO_4$ phase. The EDS study confirmed that no synthesis remnants or impurities are left in the sample which only consists of cerium, phosphorus and oxygen atoms (the carbon peak is the feature of the sample holder tape).

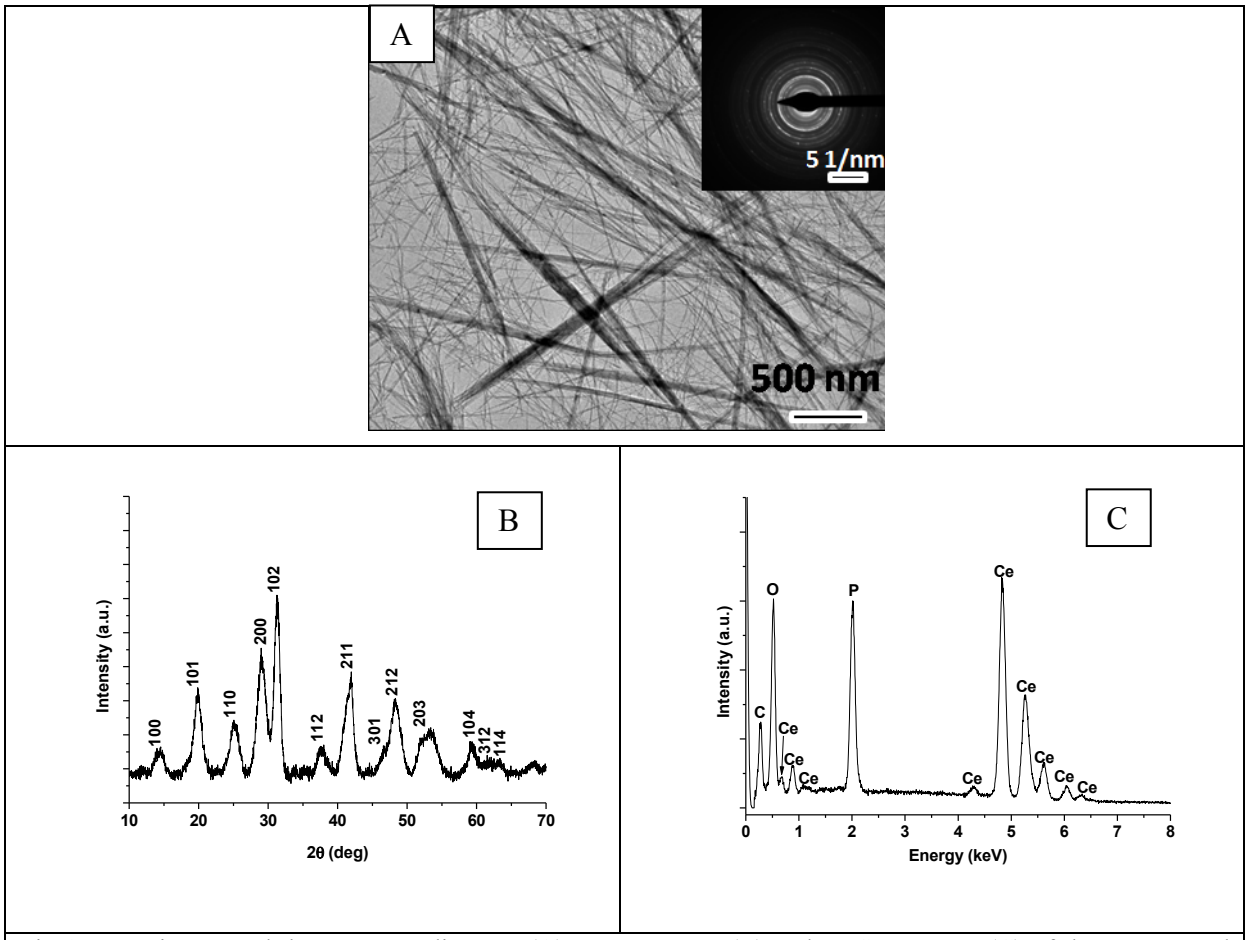

Fig 1. TEM image and the corresponding ED (A), XRD pattern (B) and EDS spectrum (C) of the as prepared $CePO_4$ nanowire sample.

The effects of calcination temperature on the structural and crystalline properties of the samples were monitored by TEM, XRD, Raman- and IR spectroscopic methods. TEM images provided the first insights to the morphological changes of the nanowires (Fig. 2). Up to 600 °C no significant changes could be observed in the samples. Raising the temperature to 800 °C initiated the structural collapse of the nanowires as the wire-like morphology started to disappear due to the sintering of the nanostructures. At higher temperature further sintering took place and at 1000 °C the sample mainly consisted of large, irregularly shaped nanoparticles and sintered wire-like structures.

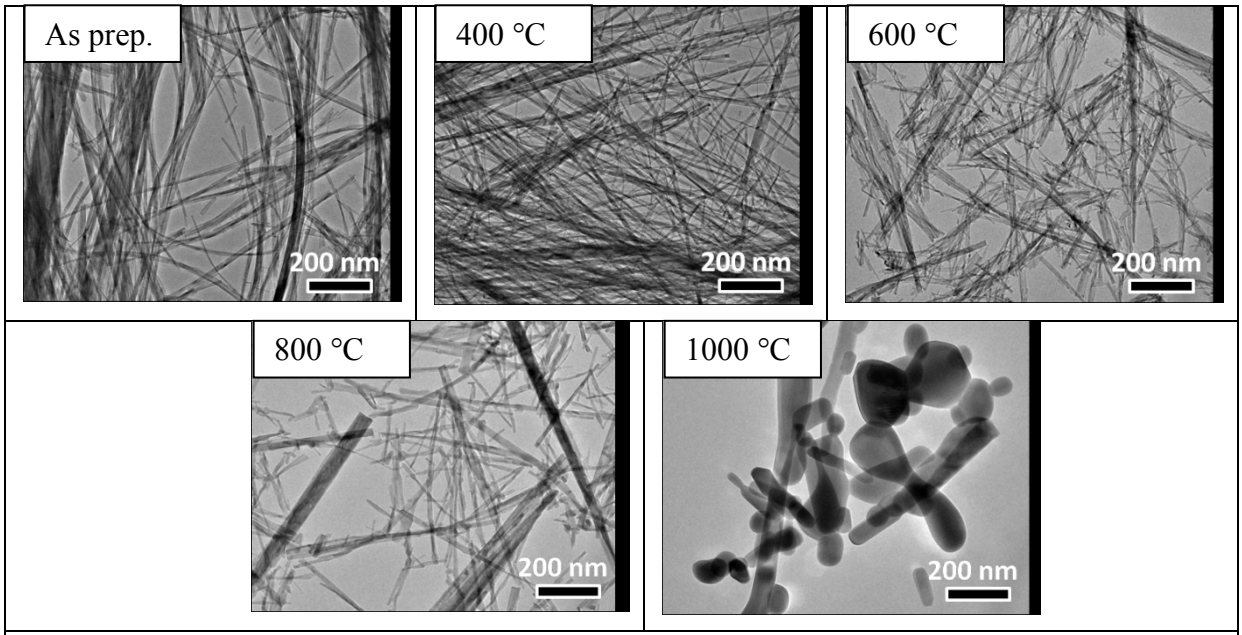

Fig 2. TEM images from morphological changes of the nanowires at different temperatures.

The specific surface area (SSA) of the samples was determined by N_2 adsorption measurements. In Fig. 3 the average nanowire diameters (as determined from TEM) and the corresponding SSA values are depicted as a function of calcination temperature. The average diameters of the samples exhibited a clear increasing tendency, accompanied by a distinct decreasing tendency in the SSAs. The as-prepared sample had an average diameter of 6.3 nm with a SSA of 148 m^2/g, whereas by calcining at 1000 °C sintered nanowires with an average diameter of 87.5 nm and SSA of 7.7 m^2/g were obtained..

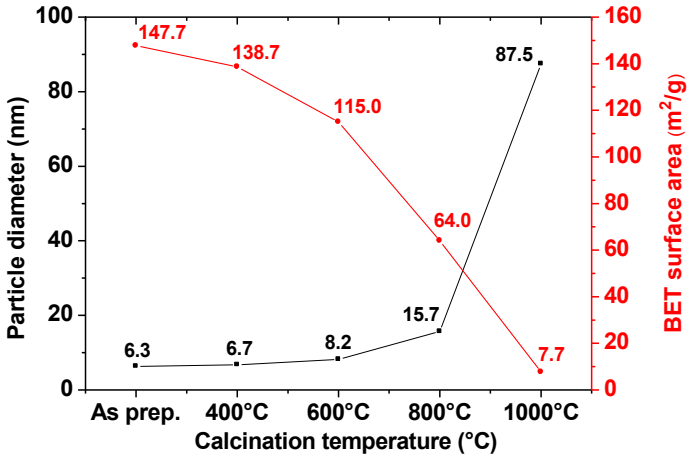

Fig. 3. Changes in specific surface area and average particle diameter in the function of calcination temperature

To investigate the phase transitions of the heat treated samples a crystallographic study was performed. XRD patterns depicted in Fig. 4 showed the recrystallization process of the nanowires from hexagonal to monoclinic phase. All the peaks of the as prepared sample can be readily indexed to the hexagonal phase of $CePO_4$ which seemed to be stable up to 400 °C. Between 400 °C and 600 °C the nanowires underwent a recrystallization process: the reflections of hexagonal phase disappeared at 600 °C and the reflections of monoclinic phase (the stable crystal form of $CePO_4$ at higher temperatures) appeared [23,25]. At 800 °C and 1000 °C no additional crystal transitions or metaphases could be observed, however, the increasing reflection intensities and decreasing full width at half maximum values (FWHMs) indicate improved crystallinity and growing average particle size previously confirmed by TEM.

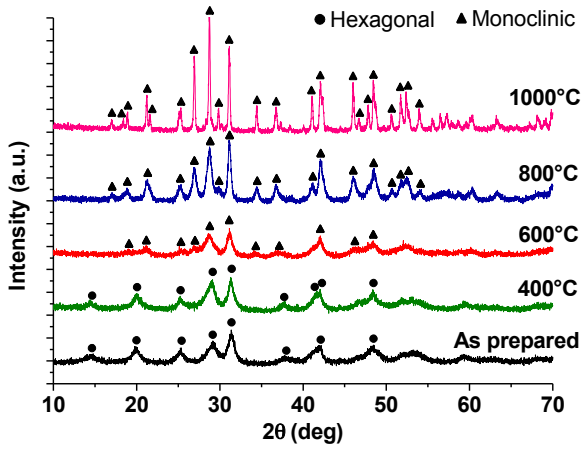

Fig. 4. XRD patterns of the calcined samples showing the recrystallization of the nanowires

Raman and IR measurements were performed to confirm the crystallographic determinations based on XRD . Fig. 5 depicts the IR spectra of the calcined nanowires. The as-prepared sample featured the vibrations of the PO_4^{3-} group in a hexagonal structure with the space group D_3^4 where the anions occupy the C_2 site symmetry.

The bands at 1051 cm^{-1} and 1020 cm^{-1} are assigned to the antisymmetric stretching vibration of the P-O bond (ν_3) while the band at 967 cm^{-1} can be assigned to the symmetric stretching vibration of P-O bond (ν_1). The vibrations at 615, 569 and 542 cm^{-1} are related to the bending modes of PO_4^{3-} group (ν_4) [26]. As the temperature was raised to 400 °C the characteristic stretching vibrations started to rearrange. The bands at 1020 and 967 cm^{-1} almost disappeared while a new band at 995 cm^{-1} appeared corresponding to the ν_1 vibration of P-O bond in monoclinic structure. This observation indicates that the structural rearrangement may commence at lower temperatures than expected on the basis of XRD results. Above 600 °C new bands appeared in the ν_3, ν_1 stretching and ν_4 bending region manifesting the total recrystallization of $CePO_4$ nanowires into the monoclinic phase [26,27].

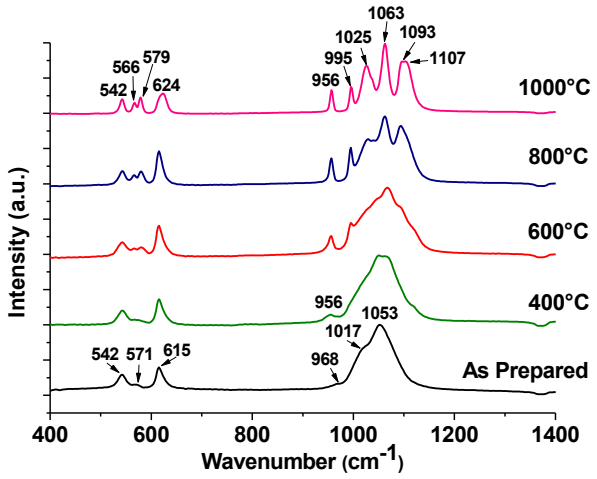

Fig. 5. IR spectra of the calcined samples representing the recrystallization of the nanowires

Raman results (Fig. 6) confirmed the IR study. The two bands at 1085 and 976 cm^{-1} in the spectrum of the as-prepared sample correspond to the symmetric and antisymmetric stretching vibrations of P-O bond. The bands in the lower region can be assigned to the bending modes of the PO_4^{3-} group from which 571 and 624 cm^{-1} vibrations are the antisymmetric ones while 466, 377 cm^{-1} vibrations are the symmetric ones [28,29]. Similarly to the observations of the IR study, the Raman spectrum of the sample calcined at 400 °C featured only two vibrations at 976 and 466 cm^{-1} representing a transitional state between the hexagonal and the monoclinic structure. Above 600 °C the bands of the PO_4^{3-} group characteristic to the monoclinic structure appeared. At 990 and 1024 cm^{-1} the antisymmetric stretching modes of the PO_4^{3-} group appeared while the bands at 1054 and 1070 cm^{-1} can be attributed to the splitting of these vibrations [30]. At 969 cm^{-1} an intense vibration related to the symmetric stretching mode of the PO_4^{3-} group can be observed. The bands at 618 – 396 cm^{-1} can be assigned to the bending vibrations of PO_4^{3-} group.

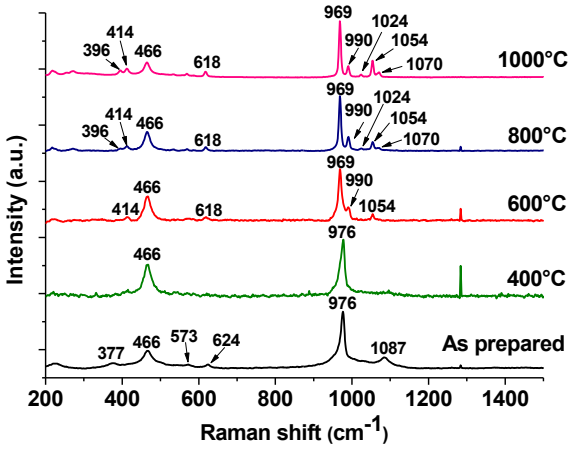

Fig. 6. Raman spectra of the calcined sample showing the recrystallization of the nanowires

4. Conclusion

In summary, a structural stability test was performed on $CePO_4$ nanowires prepared at mild ambient synthesis conditions. The samples were calcined at different temperatures and a series of measurements were performed to investigate the resulting structural changes.. According to TEM observations the nanowire morphology was stable up to 600 °C. At 800 °C a sintering process was initiated and at 1000 °C the wire-like structure collapsed. A simultaneous XRD study indicated the recrystallization of the hexagonal nanowires into a monoclinic phase at 600 °C. Interestingly, vibrational spectroscopic measurements revealed that the structural rearrangement commences at 400 °C, at a significantly lower temperature than expected solely from XRD data. This finding emphasizes the importance of supplementing XRD crystallographic studies with Raman and infrared spectroscopic local structure analysis.

Acknowledgement

The financial support of the TÁMOP-4.2.2.A-11/1/KONV-2012-0047, TÁMOP-4.2.2.A-11/1/KONV-2012-0060 and FP7 INCO „NAPEP" 266600 projects is acknowledged. The authors thank Dániel Madarász for EDS measurements and László Nagy for experimental assistance.

[1] Shanmu Dong , Xiao Chen , Lin Gu , Xinhong Zhou , Lanfeng Li , Zhihong Liu , Pengxian Han , Hongxia Xu , Jianhua Yao , Haibo Wang , Xiaoying Zhang , Chaoqun Shang , Guanglei Cui and Liquan Chen, Energy Environ. Sci., 4 (2011) 3502

[2] Guozhen Shen and Di Chen, Front. Optoelectron. China, 3 (2010) 125

[3] Gin-ya Adachi and Nobuhito Imanaka, Chem. Rev., 98 (1998) 1479

[4] Y. Liu, Richard A. Thomas, S. S. Malhotra, Z. S. Shan, S. H. Liou and D. J. Sellmyer, J. Appl. Phys. 83 (1998) 6244

[5] D.W. McKee, Carbon, 23 (1985) 707

[6] Xiaoming Liu and Jun Lin, J. Appl. Phys., 100 (2006) 124306

[7] Hoffmann C, Faure AC, Vancaeyzeele C, Roux S, Tillement O,Pauthe E and Goubard F., Anal Bioanal Chem., 399 (2011) 1653

[8] Ru Yang, Jie Qin, Min Li, Yanhong Liu and Fei Li, CrystEngComm, 13 (2011) 7284

[9] Fen Zhang and Stanislaus S. Wong, ACS Nano, 4 (2010) 99

[10] Hiroaki Onoda, Hiroyuki Nariai, Ai Moriwaki, Hideshi Maki and Itaru Motooka, J. Mater. Chem., 12 (2002) 1754

[11] Jungjin Park, Yuhong Oh, Yejun Park, Seunghoon Nam, Joonhee Moon, Joonhyeon Kang, Dae-Ryong Jung, Sujin Byun, Byungwoo Park, Current Applied Physics, 11 (2011) S2

[12] Eric H. Oelkers, Jean-Marc Montel, Elements, 4 (2008) 113

[13] M. Rappaz, M. M. Abraham, J. O. Ramey and L. A. Boatner, Phys. Rev. B, 23 (1981) 1012

[14] G. Alberti, U. Costantino, F. Di Gregorio, P. Galli and E. Torracca, J. inorg. nucl. chem., 30 (1968) 295

[15] K.G. Varshney, M.Z.A. Rafiquee and Amita Somya, Colloids and Surfaces A: Physicochem. Eng. Aspects, 301 (2007) 69

[16] Minh-Vien Lea, Dah-Shyang Tsaia, Chia-Ying Yanga, Wen-Hung Chunga and Hsin-Yi Lee, Electrochimica Acta, 56 (2011) 6654

[17] Cuicui Yu, Min Yu, Chunxia Li, Xiaoming Liu, JunYang, Piaoping Yang and Jun Lin, Journal of Solid State Chemistry, 182 (2009) 339

[18] Yan Xing, Mei Li, Sean A. Davis and Stephen Mann, J. Phys. Chem. B, 110 (2006) 1111

[19] Wenbo Bu, Zile Hua, Hangrong Chen and Jianlin Shi, J. Phys. Chem. B, 109 (2005) 14461

[20] Yu Wenyuan, Li Guanlai and Zhou Li, Journal of Rare Earths, 28 (2010) 171

[21] Yue-Ping Fang, An-Wu Xu and Wen-Fei Dong, small, 1 (2005) 1967

[22] Jinrong Bao, Ranbo Yu, Jiayun Zhang, Dan Wang, Jinxia Deng, Jun Chena and Xianran Xinga, Scripta Materialia, 62 (2010) 133

[23] Adly Abdella Hanna, Sahar Mohamed Mousa, Gehan Mahmoud Elkomy and Marwa Adel Sherief, European Journal of Chemistry, 1 (2010) 211

[24] I. Szczygiel, T. Znamierowska, Journal of Thermal Analysis and Calorimetry, 36 (1990) 2195

[25] Li Bo, Shen Liya, Liu Xiaozhen, Wang Tianmin, K. Ishii, Y. Sasaki, Y. Kashiwaya, H. Takahashi and T. Shibayama, Journal of Materials Science Letters, 19 (2000) 343

[26] A. Hezel and D. Ross, Spectrochimica Acta, 22 (1966) 1949

[27] Toshiyuki Masui, Hiroshi Tategaki, Shinya Furukawa and Nobuhito Imanaka, Journal of Ceramic Society of Japan 112 (2004) 646

[28] D. Uy, A.E. O'Neill, L. Xu, W.H. Weber and R.W. McCabe, Applied Catalysis B: Environmental 41 (2003) 269

[29] H. Assaaoudi, A. Ennaciri, A. Rulmont, Vibrational Spectroscopy, 25 (2001) 81

[30] G.M. Begun, C.E. Bamberger, J. Raman Spectrosc. 13 (1982) 284